

## ***In Situ* X-Ray Reflectivity and Diffraction Studies of the Au(001) Reconstruction in an Electrochemical Cell**

B. M. Ocko and Jia Wang

*Physics Department, Brookhaven National Laboratory, Upton, New York 11973*

Alison Davenport and Hugh Isaacs

*Department of Applied Science, Brookhaven National Laboratory, Upton, New York 11973*

(Received 31 May 1990)

*In situ* x-ray specular reflectivity and glancing-incident-angle x-ray diffraction measurements have been performed at the Au(001) surface in a 0.01M HClO<sub>4</sub> solution under potential control in an electrochemical cell. At -0.4 V versus an Ag/AgCl electrode, the gold surface exhibits a hexagonal reconstructed layer with a mass density 21% greater than the underlying bulk layers. The reconstruction disappears above 0.5 V, and the excess atoms form a new atomic layer with a density corresponding to 22% of a bulk layer. The reconstruction fully recovers below -0.3 V.

PACS numbers: 61.10.-i, 82.45.+z

Most structural studies of metal surfaces have been performed under UHV conditions where temperature is the independent thermodynamic variable. In an electrochemical environment, the electric field or charge at the surface can be controlled by changing the potential across the polarized "double layer."<sup>1</sup> For a given potential, the surface electric field can be calculated from the Gouy-Chapman-Stern model, the one-dimensional analog of the Poisson-Boltzmann equation, from the concentration of ions in the electrolyte.<sup>1</sup> Electric fields as high as 10<sup>7</sup> V/cm across the double layer are accessible and the corresponding change in surface charge can easily exceed 0.1 electron per surface atom. In vacuum, adsorbates can induce an external electric field which alters the surface charge and thus the surface structure.<sup>2</sup> For instance, the missing-row (2×1) surface structure, which exists for clean (110) surfaces of Pt and Au, can be induced for Ag by the adsorption of alkali metals.

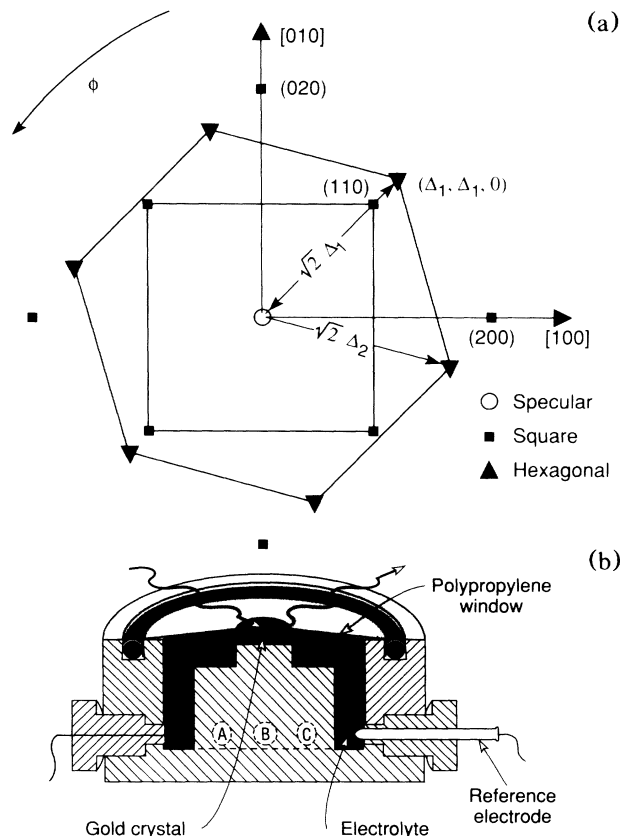
The understanding of surface structure in vacuum has progressed rapidly over the last several decades; many of the developments have been due to techniques involving electron probes. In electrochemistry, electrode surfaces are of fundamental importance, yet, very little is known about their *in situ* structure. In part, this is due to the inability of electrons to penetrate solutions. With the availability of high-brightness synchrotron sources, surface x-ray diffraction has become a viable method to study *in situ* structure.<sup>3,4</sup>

The present study has been motivated by extensive electrochemical studies of the Au(001) surface.<sup>5,6</sup> Cyclic voltammetry of the Au(001) surface in HClO<sub>4</sub> solutions exhibits an anodic current peak at ~0.7 V versus an Ag/AgCl electrode. From measurements of the potential of zero charge (PZC)<sup>5,6</sup> which is related to the work function,<sup>7</sup> optical reflectivity (OR),<sup>6</sup> and second-harmonic generation,<sup>8</sup> it has been inferred that a potential change can induce a surface structural transition. *Ex situ* low-energy electron-diffraction measurements, after emersion from an electrochemical cell,<sup>9</sup> suggest

that the structural transition inferred from the PZC and OR corresponds to the lifting of the hexagonal reconstruction. In this Letter, we present an x-ray reflectivity and surface x-ray diffraction study of the Au(001) surface reconstruction in a HClO<sub>4</sub> solution under potential control.

In vacuum, the Au(001) surface exhibits a hexagonal reconstruction<sup>10-13</sup> where there are nearly six surface atoms for every five bulk atoms along the [110] direction. The reconstruction is often referred to as "5×20" although the actual top layer is more accurately described as incommensurate.<sup>12</sup> The in-plane surface diffraction [see Fig. 1(a)] is described by a hexagonal pattern centered around the origin with a wave vector  $\sqrt{2}\Delta_1 a^*$  ( $\Delta_1 = \Delta_2$ ), where the incommensurability  $\delta = \Delta_1 - 1 = 0.206 \pm 0.001$ ,<sup>11,14</sup>  $a^* = 2\pi/a$ , and  $a = 4.081 \text{ \AA}$  is the size of the face-centered-cubic unit cell for Au. The orientation of the reconstructed layer is rotated by  $\pm 0.8^\circ$  from the [110] axis,<sup>13</sup> with a surface corrugation amplitude of  $\lesssim 0.50 \text{ \AA}$  peak to peak,<sup>12,14,15</sup> a 25% excess mass relative to the underlying bulk layers,<sup>16,17</sup> and a 20% interlayer expansion.<sup>17</sup> The excess mass and the expansion nearly conserve the bulk packing density.

*In situ* measurements were made with gold disk electrodes (2 mm by 10 mm diameter) prepared from single-crystal rods. The rods were spark cut, aligned within 0.1° to the crystallographic axis, sanded and polished down to 1  $\mu\text{m}$ , and electropolished and sputtered in Ar at  $P = 5 \times 10^{-5}$  Torr at 800°C. The samples were transferred in air to the cylindrical Kel-F electrochemical cell [Fig. 1(b)]. The potential applied to the Au(001) sample is referenced to a Ag/AgCl (3M KCl) electrode connected to the cell through a microglass frit to minimize chloride contamination. Superpure HClO<sub>4</sub> (Merck) was diluted with ultrapure H<sub>2</sub>O (Millipore Corp.) to 0.01M and deoxygenated with 99.999% N<sub>2</sub> gas (Matheson). A 6- $\mu\text{m}$  polypropylene window covers and seals the cell with a thin capillary electrolyte film (< 20  $\mu\text{m}$ ) between the crystal face and the polypropylene film.



### ELECTROCHEMICAL X-RAY SCATTERING CELL

FIG. 1. (a) In-plane diffraction pattern for the Au(001) surface. Each point represents a rod of scattering normal to the surface. (b) Electrochemical x-ray scattering cell. A, electrolyte input; B, Pt counter electrode; C, electrolyte output.

An outer chamber is flushed with  $N_2$  gas to maintain deaeration.

X-ray measurements were carried out with focused monochromatic radiation,  $\lambda = 1.243 \text{ \AA}$  at the X22C beam line of the National Synchrotron Light Source using a four-circle diffractometer. The scattering vector  $\mathbf{Q}$  is represented in terms of the Miller indices  $(H, K, L)$ , where  $H = (a/2\pi)Q_x$ ,  $K = (a/2\pi)Q_y$ , and  $L = (a/2\pi) \times Q_z$ . For specular reflectivity the longitudinal resolution,  $\Delta Q_z = 0.008 \text{ \AA}^{-1}$  HWHM (half width at half maximum), is set by the detector slits. Absolute reflectivity was obtained by integrating the specular signal, at each  $L$ , in a  $1^\circ \theta$  rocking curve.<sup>17</sup> In Fig. 2, the reflectivity data are shown at controlled potentials of  $-0.4 \text{ V}$  (open circles) and  $1.0 \text{ V}$  (solid circles). There is a significant difference between the behavior of the reflectivity spectrum at these two potentials. This is most apparent near the (001) position where the reflectivity at  $-0.4 \text{ V}$  is nearly a factor of 5 higher than at  $1.0 \text{ V}$ . Neither of these data sets agrees with the model for ideal termination, shown by the long-dashed line in Fig. 2.

The specular reflectivity  $R(Q_z)$  can be described as a

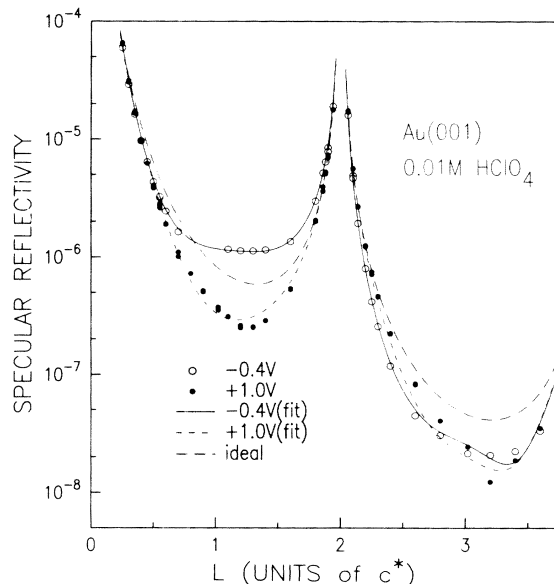


FIG. 2. Absolute reflectivity data for the  $(0,0,L)$  rod at 300 K for  $-0.4 \text{ V}$  (open circles) and  $1.0 \text{ V}$  (solid circles), where  $L = (a/2\pi)Q_z$ . The long-dashed line is for ideal termination with no rms displacement amplitude. The solid and short-dashed lines are fits as described in the text.

simple sum over the atomic layers,<sup>14,17</sup>

$$R(Q_z) = \left| \frac{T^2(Q_z)F(Q_z)e^{-W(Q_z)}}{Q_z} \right|^2 \left| \frac{2\pi r_0}{a^2} \right|^2 e^{-Q_{\text{abs}}/Q_z} \times \left| \sum_{m=0}^{\infty} \langle \rho_m e^{-Q_z^2 \sigma_m^2 / 2} e^{iQ_z (a/2)(m - \epsilon_m)} \rangle \right|^2, \quad (1)$$

where  $W(Q_z)$  is the Debye-Waller factor,  $T$  is the Fresnel surface-enhancement factor,  $F$  is the atomic form factor,  $r_0$  is the Thomson radius, and  $Q_{\text{abs}} \cong 0.22 \text{ \AA}^{-1}$  is an absorption correction at small  $Q_z$  originating from the window and the electrolyte. Each term in the sum corresponds to an atomic layer ( $m$ ), where  $\rho_m$  is the electron density relative to a bulk (001) layer,  $\epsilon_m$  is the increase in the atomic layer spacing relative to bulk (001) layers, and  $\sigma_m$  is the root-mean-square (rms) atomic displacement. The rms factor includes the effects of corrugation and enhanced surface vibrations.<sup>14</sup> Scattering from solution species does not significantly affect the reflectivity after background subtraction.

The specular reflectivity, over the range  $0.2 < L < 3.5$ , has been fitted by Eq. (1). At  $-0.4 \text{ V}$  an excellent fit (Fig. 2, solid line) is obtained with a top-layer density  $\rho_1 = 1.21$  ( $\rho_0 = 0$ ), a relative interlayer expansion between the hexagonal top layer and the next gold layer of  $\epsilon_1 = 0.20$ , and an enhancement of the rms displacement amplitude  $\sigma_{(1-3)} = 0.50, 0.16, \text{ and } 0.09 \text{ \AA}$ . The excess density and expansion of the top layer are in close agreement with a dense-packed hexagonal layer as observed in vacuum.<sup>17</sup> The increase in the fitted value of the top-layer rms amplitude,  $\sigma_1 = 0.50 \text{ \AA}$  relative to the corresponding room-temperature vacuum value,<sup>14</sup>  $0.30 \text{ \AA}$ ,

suggests that the electrochemically reconstructed surface is rougher, i.e., more buckled. For 1.0 V, the best fit is obtained with a top-layer density  $\rho_0=0.22$  and all other layers with unity density. The density of this top layer ( $m=0$ ) is within errors equivalent to the excess mass of the reconstructed phase ( $m=1$ ), i.e.,  $\rho_1(-0.4 \text{ V}) - 1 = \rho_0(1.0 \text{ V})$ . The only additional parameters in the analysis at 1.0 V are the rms atomic displacements of the top three layers,  $\sigma_{(0-2)}=0.48, 0.15, 0.08 \text{ \AA}$ . If the density of all the layers is constrained to be unity, the goodness of fit parameters  $\chi^2$  increases by a factor of 10. This is rather convincing evidence that the top layer contains only a small fraction of the atoms relative to an underlying bulk (001) atomic layer.

The density of each atomic layer [Eq. (1)] is the local atomic density averaged over the coherence area of the x-ray resolution function. For the present measurements the coherence area is  $\pi^2/(\Delta Q_x \Delta Q_y) \cong 60 \times 20 \text{ \AA}^2$  at  $L=2$ . If the excess surface atoms at 1.0 V were to segregate at steps with a  $1 \times 1$  structure and with a terrace size much greater than the x-ray coherence area, then the observed top-layer density would be unity. This is not the case. Instead, the surface atoms either form small islands,<sup>18</sup> with amorphous phase, or an ordered array such as a  $2 \times 2$  structure.<sup>19</sup> Between 0.5 and 1.0 V there is virtually no change in the specular reflectivity profiles.

Measurements of the in-plane diffraction were carried out at  $L=0.3$  to obtain the best signal-to-background ratio. In order to reduce stray scattering from the gold sample, the window, and the electrolyte, 10-mrad Soller slits were utilized to provide in-plane collimation ( $\Delta Q_{\parallel}=0.013 \text{ \AA}^{-1}$  HWHM). At negative potentials, the in-plane diffraction features a near hexagonal pattern with  $\Delta_1=1.205 \pm 0.002$  and  $\Delta_2=1.200 \pm 0.005$ , where  $\Delta_1$  and  $\Delta_2$  are the hexagonal wave vectors along the (110) and rotated directions shown in Fig. 1(a). The initial measurements were carried out directly after placing the sample in the cell and filling with 0.01M HClO<sub>4</sub> acid while holding the potential at  $-0.4 \text{ V}$ . A central peak at (1.205, 1.205, 0.3) in the rocking curve is observed (Fig. 3, solid circles). At sufficiently positive potentials the reconstruction is lifted. Subsequent potential cycles to  $-0.4 \text{ V}$  no longer display a central peak in the rocking curves, but rather two peaks rotated by  $0.8^\circ$  as shown by the open circles. The rotation and the incommensurability  $\delta=0.205$  are in near perfect agreement with vacuum studies of the Au(001) surface.<sup>12,13</sup> In contrast to the vacuum studies where the hexagonal domain along the (110) direction is as intense as the rotated domains, no strong central domain is observed.

The rocking-curve widths of the surface peaks are slightly broader than the in-plane mosaic ( $\sim 0.25^\circ$  HWHM) which is shown in Fig. 3 at (1,1,0.3) as squares. The longitudinal scan for the  $(\Delta_1, \Delta_1, 0.3)$  peak is 50% broader than the in-plane resolution  $\Delta Q_{\parallel}$ , and the calculated length of the reconstructed regions is at least

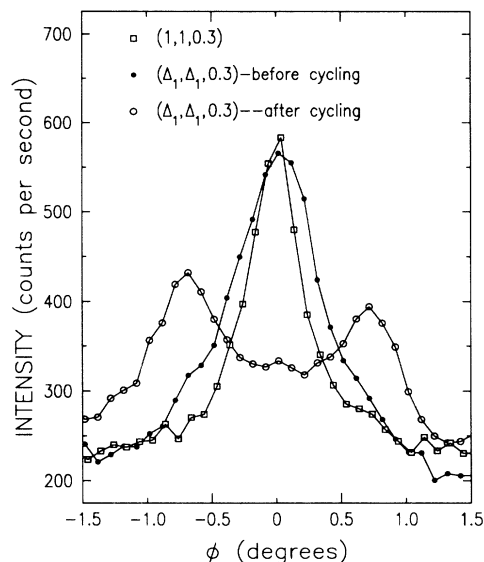


FIG. 3. Glancing-incident-angle x-ray-diffraction rocking curve at  $L=0.3$  and  $-0.4 \text{ V}$ . The scan at  $(\Delta_1, \Delta_1, 0.3)$  before cycling the potential (solid circles) is aligned along the (1,1,0) axis. After the potential is cycled to 1.0 V and back to  $-0.4 \text{ V}$ , rotated domains,  $\pm 0.8^\circ$ , are present (open circles). The rocking curve at (1,1,0.3) intersects the bulk truncation rod (squares).

$300 \text{ \AA}$ . We note that the domain size of the hexagonal phase is much greater than the spectrometer coherence area for the reflectivity measurements. From the in-plane diffraction study, the structure of the low-density overlayer at potentials where the hexagonal order vanishes cannot be determined. If an ordered low-density top layer exists, the scattering would be  $\sim (0.22/1.22)^2 = 3\%$  of the scattering intensity from the dense reconstructed layer. This would be nearly impossible to detect with the current signal-to-background ratio.

In Fig. 4(a), the potential dependence of the reconstruction peak at  $(\Delta_1, \Delta_1, 0.3)$  with increasing potential is shown. Note that the integrated intensity of the hexagonal surface reflection is constant up to 0.2 V and that the intensity decreases to half of the maximum intensity at 0.35 V. Data were obtained in steps for an effective scan rate of 0.004 mV/sec. This rate is a factor of 10000 slower than those rates typically used for cyclic voltammetry.<sup>6</sup> If the rate is increased to 0.1 mV/sec the transition occurs at 0.5 V. The integrated intensity of the  $(\Delta_1, \Delta_1, 0.3)$  peak has been investigated as a function time by stepping the potential from the steady-state  $-0.5 \text{ V}$  regime to 0.5, 0.6, and 0.75 V. At 0.5 V the intensity decreases to 30% after 60 min and to 10% after 100 min. At 0.6 and 0.75 V the intensity decreases to 10% within 1 min and vanishes after several minutes. This behavior is consistent with cyclic-voltammetry measurements<sup>6</sup> in which an anodic current peak is observed at 0.70 V versus Ag/AgCl at scan rates of 50 mV/sec. The behavior of the hexagonal peaks rotated by  $60^\circ$ , see Fig. 1(a),

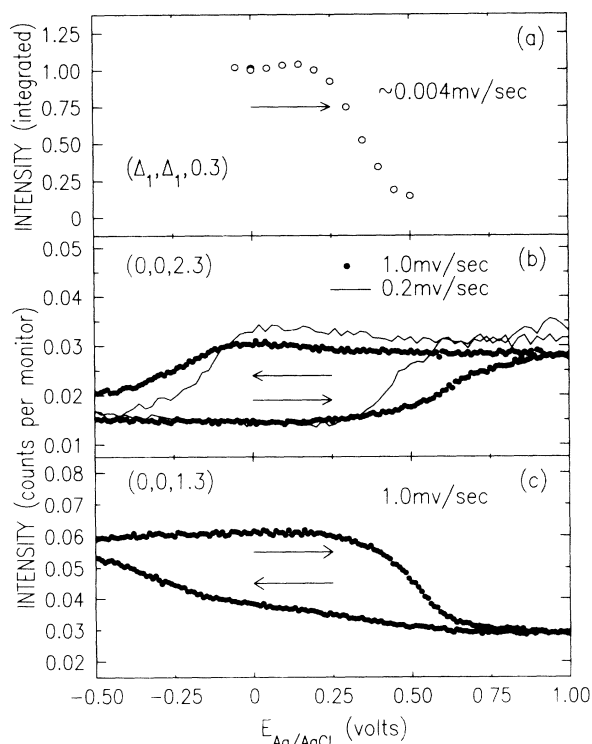


FIG. 4. Potential dependence of the surface scattering from Au(001) in 0.01M HClO<sub>4</sub>. (a) Integrated intensity of the hexagonal reconstruction peak for Au(001), ( $\Delta_1, \Delta_1, 0.3$ ), for increasing voltages. (b) Peak intensity at (0,0,2.3) vs voltage at several scan rates. (c) Peak intensity at (0,0,1.3) vs voltage at 1.0 mV/sec.

versus potential agrees with the scattering at ( $\Delta_1, \Delta_1, 0.3$ ).

In the lower two panels of Fig. 4 the voltage dependence of the intensity of the scattering is shown at (0,0,1.3) and (0,0,2.3). All of the cycles were initiated after steady state was achieved at  $-0.5$  V. Scans at (0,0,1.3) are more sensitive to roughness effects, whereas at (0,0,2.3) layer expansion plays a more pivotal role. Differences in the intensity versus potential are clearly observed for scan rates of 0.2 and 1.0 mV/sec. This behavior is consistent with the slow kinetics of the potential-step measurements ( $-0.5$  to  $0.5$  V) reported above. The hexagonal reconstruction starts to form at a much lower potential ( $\sim 0.0$  V) than the disappearance of the hexagonal reflections as shown in Fig. 4(b) at (0,0,2.3). In part, this irreversibility is due to a 0.22-V shift in the unreconstructed-phase PZC (0.12 V) relative to the reconstructed PZC (0.34 V).<sup>20</sup> From the integrated-intensity measurements of the ( $\Delta_1, \Delta_1, 0.3$ ), a significant increase in the in-plane order was only observed below  $-0.2$  V. At  $-0.3$  V, 70% of the intensity recovers after 3–6 min and 90% of the intensity recovers in 20–30 min. The reconstruction recovery time increases when the sample is held for longer periods at 1.0 V where the low-density top-layer phase is present. This kinetic effect suggests that the low-density phase may indeed correspond to small monolayer islands.

These measurements conclusively demonstrate that important structural information on electrode surfaces can be obtained from *in situ* surface x-ray scattering experiments. In 0.01M HClO<sub>4</sub> the hexagonal structure of the Au(001) surface at  $-0.4$  V is nearly identical to room-temperature vacuum results both in the surface plane and along the surface normal directions. At high potentials we observe a transition to a low-density top-layer phase of monolayer islands. The transition between these two phases exhibits hysteretic behavior because of the shift in the PZC and partly because of kinetic effects. Future experiments will explore the role of surface morphology, trace impurities, and different electrolytes.

We have benefited from discussions with Hector Abruna, John Axe, Chris E. D. Chidsey, Doon Gibbs, Joe Gordon, Jim McBreen, Simon Mochrie, Ian Robinson, Michael Toney, and David Zehner. This work has been supported by an exploratory research grant at Brookhaven National Laboratory and by the Division of Materials Research, U.S. Department of Energy, under Contract No. DE-AC02-76CH00016.

<sup>1</sup>A. J. Bard and L. R. Faulkner, in *Electrochemical Methods* (Wiley, New York, 1980).

<sup>2</sup>C. L. Fu and K. M. Ho, Phys. Rev. Lett. **63**, 1617 (1989).

<sup>3</sup>O. R. Melroy, M. F. Toney, G. L. Borges, M. G. Samant, L. Blum, J. B. Kortright, P. N. Ross, and L. Blum, Phys. Rev. B **38**, 10962 (1988).

<sup>4</sup>M. G. Samant, M. F. Toney, G. L. Borges, L. Blum, and O. R. Melroy, J. Phys. Chem. **92**, 220 (1988).

<sup>5</sup>A. Hamelin, J. Electroanal. Chem. **142**, 299 (1982).

<sup>6</sup>D. M. Kolb and J. Schneider, Surf. Sci. **162**, 764 (1985).

<sup>7</sup>J. O'M. Bockis and A. K. N. Reddy, in *Modern Electrochemistry* (Plenum, New York, 1970), Vol. II.

<sup>8</sup>A. Friedrich, B. Pettinger, D. M. Kolb, G. Lupke, R. Steinhoff, and G. Marowsky, Chem. Phys. Lett. **163**, 123 (1989).

<sup>9</sup>M. S. Zei, G. Lehmpfuhl, and D. M. Kolb, Surf. Sci. **221**, 23 (1989).

<sup>10</sup>P. W. Palmberg and T. N. Rhodin, Phys. Rev. **161**, 586 (1967).

<sup>11</sup>G. E. Rhead, J. Phys. F **3**, L53 (1973).

<sup>12</sup>S. G. J. Mochrie, D. M. Zehner, Doon Gibbs, and B. M. Ocko, Phys. Rev. Lett. **64**, 2925 (1990).

<sup>13</sup>Doon Gibbs, B. M. Ocko, D. M. Zehner, and S. G. J. Mochrie, Phys. Rev. B (to be published).

<sup>14</sup>B. M. Ocko, Doon Gibbs, K. G. Huang, D. M. Zehner, and S. G. J. Mochrie (to be published).

<sup>15</sup>K. H. Rieder, T. Engel, R. H. Swendsen, and M. Manninen, Surf. Sci. **127**, 223 (1983).

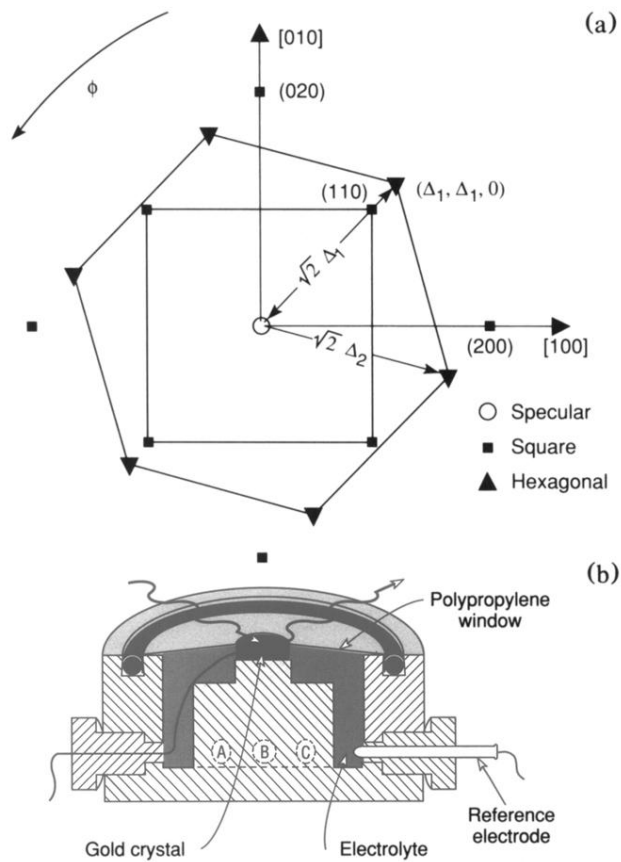
<sup>16</sup>D. M. Zehner, B. R. Appleton, T. S. Noggle, J. W. Miller, J. H. Barret, L. H. Jenkins, and O. E. Schow, III, J. Vac. Sci. Technol. **12**, 454 (1975).

<sup>17</sup>Doon Gibbs, B. M. Ocko, D. M. Zehner, and S. G. J. Mochrie, Phys. Rev. B **38**, 7303 (1988).

<sup>18</sup>W. Hosler, E. Ritter, and R. J. Behm, Ber. Bunsenges, Phys. Chem. **90**, 205 (1986).

<sup>19</sup>M. S. Zei and D. Weick, Surf. Sci. **208**, 425 (1989).

<sup>20</sup>D. M. Kolb and J. Schneider, Electrochim. Acta **31**, 929 (1986).



**ELECTROCHEMICAL X-RAY SCATTERING CELL**

FIG. 1. (a) In-plane diffraction pattern for the Au(001) surface. Each point represents a rod of scattering normal to the surface. (b) Electrochemical x-ray scattering cell. *A*, electrolyte input; *B*, Pt counter electrode; *C*, electrolyte output.